



## Photocatalytic performance of activated carbon-supported mesoporous titanium dioxide

Samira Bagheri<sup>a,\*</sup>, Zul Adlan Mohd Hir<sup>a</sup>, Amin Termeh Yousefi<sup>b</sup>,  
Sharifah Bee Abd Hamid<sup>a</sup>

<sup>a</sup>Nanotechnology and Catalysis Research Centre (NANOCAT), University of Malaya, IPS Building, Kuala Lumpur 50603, Malaysia, Tel. +60 0379676959; emails: [samira\\_bagheri@um.edu.my](mailto:samira_bagheri@um.edu.my) (S. Bagheri), [zuladlan@gmail.com](mailto:zuladlan@gmail.com) (Z.A. Mohd Hir), [sharifah@um.edu.my](mailto:sharifah@um.edu.my) (S.B. Abd Hamid)

<sup>b</sup>ChECA IKohza, Dept. Environmental & Green Technology (EGT), Malaysia Japan International Institute of Science (MJIIIT), University Technology Malaysia (UTM), Kuala Lumpur, Malaysia, Tel. +60 125185030; email: [at.tyousefi@gmail.com](mailto:at.tyousefi@gmail.com)

Received 28 October 2014; Accepted 31 March 2015

### ABSTRACT

The photocatalytic activity of methyl orange (MO) in aqueous solution was studied using the hydrothermal synthesis of activated carbon-loaded TiO<sub>2</sub> at different weight ratios. The hydrothermal process was conducted at a temperature of 180°C for 12 h in order to obtain a high surface area and porosity for the purpose of degradation activity. The results indicated that TiO<sub>2</sub>-PEG-Ac (0.50%) exhibited better photocatalytic performance compared to other prepared photocatalysts. The photodegradation process was observed to be pH dependent, since almost 100% of MO removal was possible in an acidic medium. In contrast, the degradation activity seems to be diminished in basic media. The overall photocatalytic activity of TiO<sub>2</sub> was enhanced due to the presence of porous activated carbon as co-catalyst and support.

*Keywords:* Mesoporous titania; Hydrothermal; Methyl orange; Amorphous carbon; Heterogeneous catalyst

### 1. Introduction

Photocatalytic degradation of environmental pollutants via semiconductor photocatalyst has been extensively researched over the last decade. Numerous semiconductor oxides have been introduced into the catalytic system by means of advanced oxidation process; the main goal being to eliminate the contaminant in polluted water systems effectively [1]. Among various semiconductor oxides, titania (TiO<sub>2</sub>) was found to be the most promising, due to its high

chemical stability, non-toxicity, cost effectiveness, as well as excellent photoresponse activity towards ultraviolet (UV) light [2–5]. Moreover, mesoporous materials such as titania are of great interest due to its high surface area and ability to interact with atoms, molecules, and ions, not only at their surfaces, but throughout the bulk matrices of the material [6,7]. Theoretically, a photocatalytic reaction happens when the organic substrates are attacked by radical species, such as ·OH, ·O<sub>2</sub><sup>-</sup>, and HOOH, which are produced on the surface of titania nanoparticles via the reduction of dissolved oxygen in aqueous solution and/or oxidation of surface hydroxyl of TiO<sub>2</sub> [8–12].

\*Corresponding author.

For the selected contaminant to be degraded, it is vital that the catalyst is active via light absorption for both UV and visible regions. Since anatase titania possesses a large band gap energy of 3.20 eV, the catalyst is capable of adsorbing light, mainly photons, in the UV region ( $\lambda < 387$  nm), in order to experience photoexcitation of electrons and holes. Nevertheless, high consumptions of energy from the UV-light lamp rendered the photocatalysis system to suffer from higher implementation costs. Therefore, it is important that the available and cheap solar light be used as the energy source to treat contaminated water. The invisible region, or solar light, only contain about 5% of UV energy, caused a problem for the current titania produced. In order to overcome this problem, an improvement is in order via the modification of the surface of anatase titania and its band gap energy so that the catalyst will be effective for the absorption of photons in solar light ( $\lambda > 400$  nm) [13–15].

Previously, a number of approaches for titania modification have been introduced, such as doping with transition metals (Cu, Mn, Mo, Fe, V, Nb, Co, Cr, Ni, Au, Ag, Ru, and Pt) and non-metals doping (C, N, S, P, I, F, and B) [15–21]. The surface modification of titania is crucial, as it increases the catalytic efficiency by increasing its specific surface area, pore size, and adsorption ability towards the degradation of organic pollutants. Recently, research discovered that activated carbon (Ac) possesses all these characteristics, and have been recognized as one of the promising material to be incorporated into the surface of the titania nanoparticles. The combination greatly affected the efficiency of the photocatalyst by presenting high reactivity and chemical stability in water recovery process due to the synergistic effect between the activated carbon and titania itself [22–27].

In this study, we examined the morphology and structure of meso-TiO<sub>2</sub>-loaded activated carbon via various characterization techniques. The mesoporous titania was synthesized by a combination of simple sol–gel and hydrothermal method, and the addition of activated carbon was done according to different weight ratios. The catalytic efficiency was tested in the photocatalytic degradation of aqueous methyl orange (MO) with UV lamps.

## 2. Experimental

### 2.1. Materials

Titanium isopropoxide (Ti[OCH(CH<sub>3</sub>)<sub>2</sub>]<sub>4</sub>, TTIP, 97%) was purchased from Sigma-Aldrich, and used as the titanium precursor for the preparation of mesoporous titania. Activated carbon was obtained from a

commercial brand (Aldrich). Absolute ethanol (99.9%) was purchased from Merck KgaA, and used as the solvent to assist in the hydrolysis of TTIP and for the preparation of all sols and solutions. MO was purchased from Merck and used as the substrate for photocatalytic activity measurement.

### 2.2. Hydrothermal synthesis of meso-TiO<sub>2</sub> loaded activated carbon

The mesoporous titania was loaded with activated carbon, and synthesized by a simple hydrothermal process. In a typical preparation, 1.7 mL of titanium isopropoxide (97%) was mixed in a drop wise manner with 9 mL of absolute ethanol [28]. This solution was denoted as a pure solution to prepare mesoporous titania, and the solution was stirred for 1 h to make sure the precursor was completely dissolved. Polyethylene glycol (PEG6000) (0.010 kg/L) was added into the first solution as a template to tune the porosity and surface area of the titania [29]. The second solution was prepared by adding the commercial activated carbon according to weight ratios of 0.25, 0.50, and 1.00%. In this solution, the calculated amount of activated carbon was dispersed in 9 mL of absolute ethanol and 18 mL deionized water, and sonicated for 30 min. After the dispersion process, the second solution was mixed with the precursor solution (with and without PEG6000), and stirred for several hours. Later, the solution was transferred into a 50 mL Teflon-lined autoclave, and undergo hydrothermal treatment at 180°C for 12 h. The solution was washed with deionized water several times, centrifuged, and dried in the oven at 80°C overnight.

### 2.3. Characterization

The fine powder of synthesized mesoporous titania loaded activated carbon was subjected to X-ray diffraction (XRD) and Raman analyses to determine the crystal phase composition and crystalline size of the mesoporous materials. Fourier transform infrared spectroscopy (FTIR) studies were carried out in the 400–4,000 cm<sup>-1</sup> frequency range in order to determine the chemical bondings of the catalysts' structure. For the infrared absorption spectra, the samples were formed into pellets with KBr, and the spectra were recorded on a BRUKER FTIR Spectrometer.

### 2.4. Photocatalytic activity

The photocatalytic reaction was conducted in a 150 mL quartz cylindrical glass, at room temperature

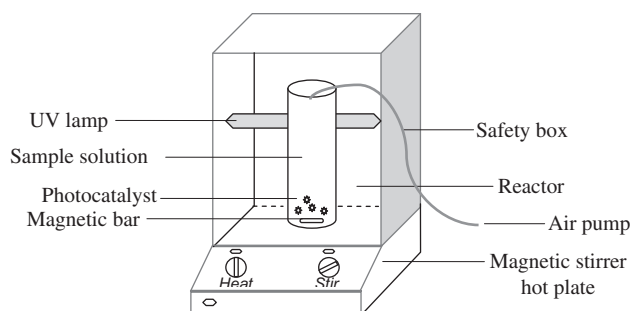


Fig. 1. The photocatalytic reactor designed for MO degradation.

and pressure. Irradiation was provided by an UV lamp with wavelength of 365 nm, located at the center of the quartz glass. A magnetic stirrer was placed at the bottom of the cylindrical glass to achieve an effective dispersion. The air was bubbled into the working solution from the bottom of the glass to ensure a constant dissolved  $O_2$  concentration (Fig. 1). To evaluate the photocatalytic efficiency, the meso- $TiO_2$ /Ac, and pure meso- $TiO_2$  powder was also tested. The amount of catalyst powder chosen was 0.5 g/L. The initial concentration of MO was 10 mg/L, and 100 mL was used for the photodegradation process. The adsorption process was performed in the presence of a catalyst under dark conditions for about 15 min prior to photodegradation activity. A sample solution of about 5 mL was withdrawn at selected time intervals, and the absorbance was measured using UV–vis spectrophotometer (UV-2501PC Shimadzu).

From the photocatalytic experiments, the percentage of MO degraded by the prepared photocatalysts was determined from the following equation (Eq. 1):

$$\% \text{ of methyl orange degradation} = \frac{C_0 - C_t}{C_0} \times 100 \quad (1)$$

where  $C_0$  is the initial concentration of MO and  $C_t$  is the concentration of MO after  $t$  min.

### 3. Results and discussion

#### 3.1. Synthesis and characterization of mesoporous $TiO_2$ -loaded activated carbon

The spectra showed that all synthesized catalysts are of the anatase phase, as reported in literature. The wavenumber appearing in the spectra is tabulated in Table 1. Comparing the Raman spectra obtained with the reference  $TiO_2$  was reported elsewhere [30], and it was clear that the Raman bands shift towards higher wavenumber have been observed (Fig. 2).

Table 1  
The wavenumber of the samples ( $cm^{-1}$ )

	$E_g$	$E_g$	$B_{1g}$	$A_{1g}$	$E_g$
$TiO_2$ -PEG	150	–	405	516	637
$TiO_2$ -without PEG	151	–	405	515	637
$TiO_2$ -PEG-Ac (0.25)	154	–	401	515	640
$TiO_2$ -PEG-Ac (0.50)	154	–	395	515	634
$TiO_2$ -PEG-Ac (1.00)	154	–	401	512	634

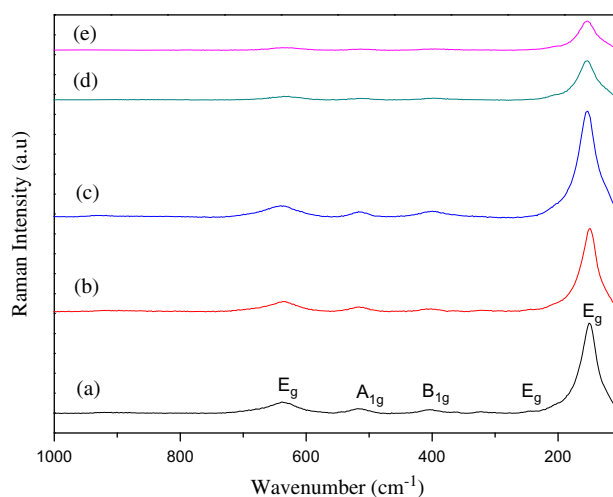


Fig. 2. Raman spectra of (a)  $TiO_2$ -PEG; (b)  $TiO_2$ -without PEG; (c)  $TiO_2$ -PEG-Ac (0.25%); (d)  $TiO_2$ -PEG-Ac (0.50%); (e)  $TiO_2$ -PEG-Ac (1.00%).

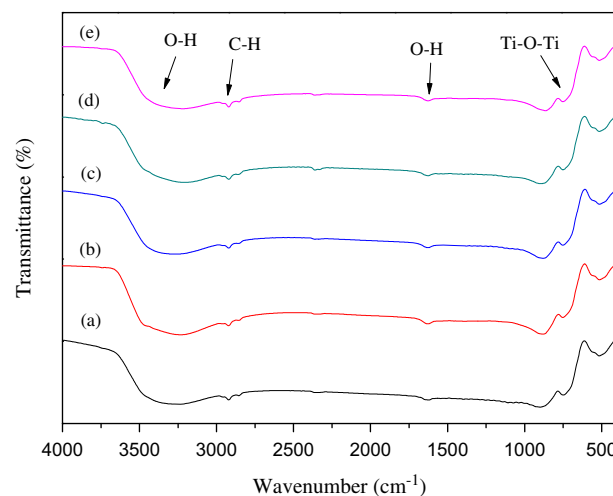


Fig. 3. FTIR spectra of (a)  $TiO_2$ -PEG; (b)  $TiO_2$ -without PEG; (c)  $TiO_2$ -PEG-Ac (0.25%); (d)  $TiO_2$ -PEG-Ac (0.50%); (e)  $TiO_2$ -PEG-Ac (1.00%).

Fig. 3 illustrates the FTIR spectra for all prepared photocatalysts used for the degradation of MO in aqueous solutions. Generally, all catalyst samples showed peaks corresponding to the stretching vibration of O–H and bending vibrations of adsorbed water molecules around  $3,200\text{--}3,400\text{ cm}^{-1}$  and  $1,600\text{ cm}^{-1}$ , respectively. The broad intense band in the range of  $450\text{--}700\text{ cm}^{-1}$  is due to the bending vibration of Ti–O–Ti bonds [31,32]. There are peaks observed at  $2,900\text{ cm}^{-1}$  for all catalyst samples regarding the C–H stretching band, which means that there are some organic compounds remaining in the catalysts' structure [33,34].

The XRD patterns of prepared photocatalysts used in this study are presented in Fig. 4. The spectra showed that the introduction of carbon material did not affect the structure of the catalyst for the formation of anatase  $\text{TiO}_2$  in the catalyst's structure. However, the intensity of the peaks decreased, probably due to a change in the crystallinity of the catalysts, in part because of the carbon compound's distribution on  $\text{TiO}_2$ 's surface. The average crystallite size of all prepared catalysts was calculated using the Debye–Scherer equation according to the XRD data obtained (JCPDS #086-1157), and is tabulated in Table 2.

### 3.2. Photocatalytic activity

Prior to the photodegradation process, the calibration curve of the targeted dye has been performed. The calibration curve was plotted according to the various concentrations of the selected dye, ranging from 1 to 10 mg/L. From this calibration plot, the linear equation

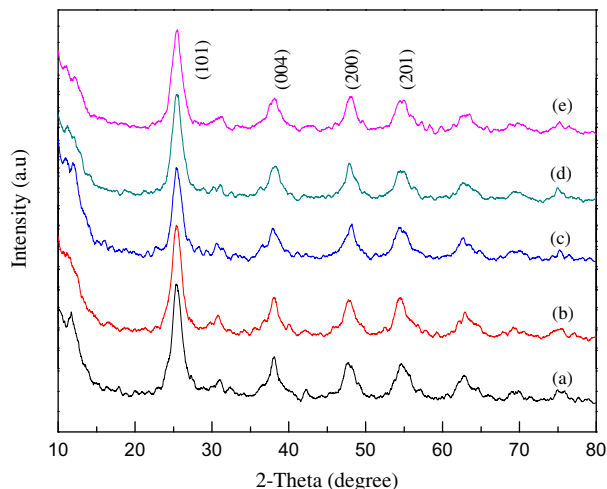


Fig. 4. XRD patterns of (a)  $\text{TiO}_2$ -PEG; (b)  $\text{TiO}_2$ -without PEG; (c)  $\text{TiO}_2$ -PEG-Ac (0.25%); (d)  $\text{TiO}_2$ -PEG-Ac (0.50%); (e)  $\text{TiO}_2$ -PEG-Ac (1.00%).

Table 2

Crystallite size of photocatalysts prepared via hydrothermal method

Catalyst	Average crystallite size (nm)
$\text{TiO}_2$ -PEG	141.61
$\text{TiO}_2$ -without PEG	148.74
$\text{TiO}_2$ -PEG-Ac (0.25%)	118.30
$\text{TiO}_2$ -PEG-Ac (0.50%)	81.36
$\text{TiO}_2$ -PEG-Ac (1.00%)	101.06

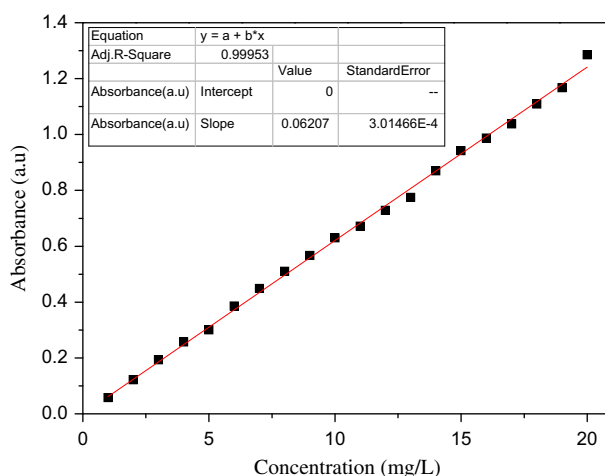


Fig. 5. Calibration plot of MO with concentration range of 1–20 mg/L.

has been determined, and can be used to evaluate the photocatalytic degradation efficiency by the prepared photocatalysts. The absorbance of each sample was measured to determine the concentration after the photodegradation process was completed (Fig. 5).

#### 3.2.1. Effect of various type of photocatalysts

The photocatalytic activity of MO (10 ppm) was performed using six different types of photocatalysts, and irradiated under UV-light lamp ( $\lambda = 365\text{ nm}$ ) for a period of 60 min. From Fig. 6, the mesoporous  $\text{TiO}_2$  photocatalyst synthesized with the addition of PEG exhibited the poorest performance, where it only resulted in a 73% of MO degradation. On the contrary,  $\text{TiO}_2$  synthesized without the addition of PEG resulted in a 84% degradation, while  $\text{TiO}_2$ -PEG-Ac (0.25),  $\text{TiO}_2$ -PEG-Ac (0.50), and  $\text{TiO}_2$ -PEG-Ac (1.00) yielded a final percentage of 83, 85, and 79%, respectively. Furthermore, the  $\text{TiO}_2$  photocatalyst loaded activated carbon without the addition of PEG resulted in 58, 54, and 55% of MO degradation, respectively. It can be concluded that the best photocatalyst in this study was

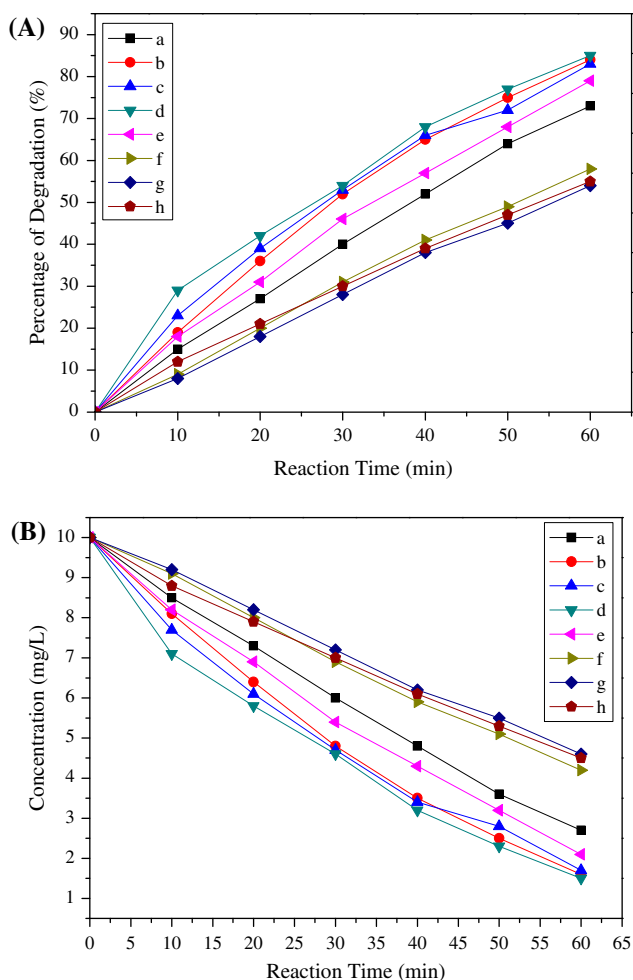


Fig. 6. (A) Percentage of photocatalytic degradation of MO for 60 min by using photocatalyst of (a) TiO<sub>2</sub>-PEG; (b) TiO<sub>2</sub>-without PEG; (c) TiO<sub>2</sub>-PEG-Ac (0.25%); (d) TiO<sub>2</sub>-PEG-Ac (0.50%); (e) TiO<sub>2</sub>-PEG-Ac (1.00%); (f) TiO<sub>2</sub>-Ac (0.25%); (g) TiO<sub>2</sub>-Ac (0.50%); (h) TiO<sub>2</sub>-Ac (1.00%) and (B) reduced concentration of the MO by those photocatalysts, [MO] = 10 ppm;  $\lambda_{UV} = 365$  nm.

TiO<sub>2</sub>-PEG-Ac (0.50%), since it exhibited better performance (~85%) from the start until 60 min of reaction times (Table 3).

The results indicated that the addition of PEG6000 into the precursor solution enhanced the performance of the photocatalyst loaded with activated carbon. It is believed that the addition of PEG could tune up the porosity and surface area of those photocatalyst, hence exhibiting better photoactivity performance than titania alone (with or without the addition of PEG). This statement is consistent with the degradation results obtained by the optimum photocatalyst of TiO<sub>2</sub>-PEG-Ac (0.50). The interfacial contact between the carbon and titania is the main factor affecting the photocatalytic activity of titania-loaded activated carbon [28].

Table 3

Percentage of degradation of MO by various photocatalysts of (a) TiO<sub>2</sub>-PEG; (b) TiO<sub>2</sub>-without PEG; (c) TiO<sub>2</sub>-PEG-Ac (0.25%); (d) TiO<sub>2</sub>-PEG-Ac (0.50%); (e) TiO<sub>2</sub>-PEG-Ac (1.00%); (f) TiO<sub>2</sub>-Ac (0.25%); (g) TiO<sub>2</sub>-Ac (0.50%); (h) TiO<sub>2</sub>-Ac (1.00%), [MO] = 10 ppm;  $\lambda_{UV} = 365$  nm

Reaction time (min)	Percentage of degradation (%)							
	a	b	c	d	e	f	g	h
0	0	0	0	0	0	0	0	0
10	15	19	23	29	18	9	8	12
20	27	36	39	42	31	20	18	21
30	40	52	53	54	46	31	28	30
40	52	65	66	68	57	41	38	39
50	64	75	72	77	68	49	45	47
60	73	84	83	85	79	58	54	55

Nevertheless, adding too much or lesser amounts of activated carbon into the precursor containing PEG solution would result in lower percentages of degradation. This study showed that the photocatalytic performance of titania-loaded activated carbon was also influenced by the preparation method. The difference in the preparation method resulted in different structural composition and synergistic interaction between titania, PEG, and activated carbon. This phenomenon significantly contributed to the different lifetime of photogenerated electron and hole pairs.

### 3.2.2. Effect of initial pH on MO degradation

The experimental results of MO degradation with varying pH of the solution in the range of 2–10 are presented in Fig. 7. The best condition for the degradation

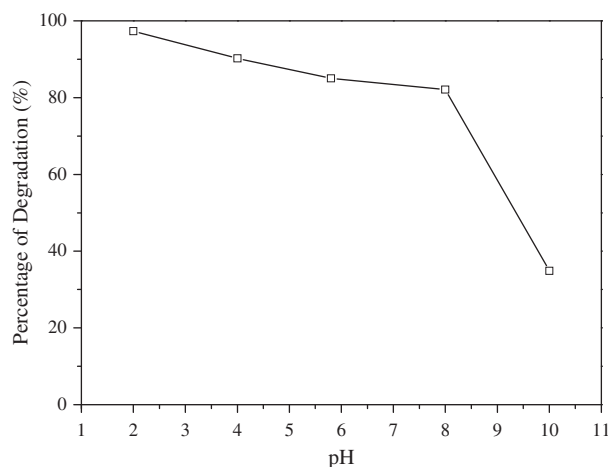


Fig. 7. The effect of various initial pH of MO solution by using 0.05 g of TiO<sub>2</sub>-PEG-Ac (0.50%), [MO] = 10 ppm;  $\lambda_{UV} = 365$  nm.

of MO compounds was obtained at pH 2 (97%) in 60 min of irradiation times. At nearly pH 6 (original pH), the percentage of degradation was reduced to 85%. In the case of TiO<sub>2</sub>-PEG-Ac (0.50%) system, the percent degradation of MO was increased as the pH was decreased from 6 to 2. Nevertheless, increasing the pH of the solution (>6) diminished the degradation ability of the respective catalyst towards MO compounds, therefore reducing the catalytic activity. Moreover, the color of MO changed from yellow to orange, and then to red in acidic conditions, due to the formation of hydrazone resonance in the structure [35].

According to Uddin et al. [36], since most of the semiconductor oxides exhibit amphoteric behavior, the pH of dispersion is the important parameter that should be accounted for in the reaction taking place on the catalyst's surface. This is because it would influence the surface charge properties of the respective catalyst used in the study. Generally, at lower pH (acidic), the surface of the catalyst is positively charged, but at higher pH (basic), it becomes negatively charged. Thus, the charged surface of the respective photocatalyst might influence the catalytic activity in degrading organic compounds, such as MO.

An article that supported these findings was reported by Kansal et al. [37], who studied the degradation of two commercial dyes (MO and Rhodamine 6G) using TiO<sub>2</sub>, SnO<sub>2</sub>, and ZnO catalysts. The alteration of the pH values of the solution influences the properties of the semiconductor–liquid interface, mainly related to the acid–base properties of the metal oxide's surface. It can be explained in terms of the zero point of charge (zpc) of the respective photocatalyst. The formation of electron hole, to adsorb the anions, is favored under conditions of pH < pH<sub>zpc</sub>.

The higher pH value reduced the number of positively charged sites and raised the number of negatively charged sites, creating electrostatic repulsion between the negatively charged surface of the TiO<sub>2</sub>-PG-Ac and the anionic MO molecules. As a result of this, there was a significant degradation of MO from the solution. Moreover, the presence of some alkali metal oxides in low vibrational modes (LVM) also provided an abundance of hydroxyl anions when the material was in contact with water, and these anions competed with the anionic MO molecules for adsorption sites, which resulted in lower degradation of MO in basic conditions [38].

#### 4. Conclusions

The effect of various catalysts prepared via hydrothermal method assisting with PEG on the photocatalytic degradation of MO was studied. The

TiO<sub>2</sub>-loaded activated carbon showed significant improvement in reactivity as compared to TiO<sub>2</sub> alone, prepared by the same method. The better photoactivity of titania loaded activated carbon nanocatalysts could be attributed to the smaller grain sizes and improved UV-light adsorption. Overall, loaded TiO<sub>2</sub> nanoparticles were found to be superior photocatalysts for rapid degradation of recalcitrant compounds, such as MO, in wastewater using UV-light as the energy source.

#### Acknowledgment

This work was supported by the University Malaya Research Grant UMRG RP022-2012A and GC001D-14AET.

#### References

- [1] R. Andreozzi, V. Caprio, I. Amedeo, R. Marotta, Advanced oxidation processes (AOP) for water purification and recovery, *Catal. Today* 53(1) (1999) 51–59.
- [2] M.R. Hoffmann, S.T. Martin, W.Y. Choi, D.W. Bahnemann, Environmental applications of semiconductor photocatalysis, *Chem. Rev.* 95 (1995) 69–96.
- [3] A.L. Linsebigler, G.Q. Lu, J.T. Yates, Photocatalysis on TiO<sub>2</sub> surfaces: Principles, mechanisms, and selected results, *Chem. Rev.* 95 (1995) 735–758.
- [4] O. Zahraa, S. Maire, F. Evenou, C. Hachem, M.N. Pons, A. Alinsafi, M. Bouchy, Treatment of wastewater dyeing agent by photocatalytic process in solar reactor, *Int. J. Photoenergy* 2006 (2006) 1–9.
- [5] A. Fujishima, T.N. Rao, D.A. Tryk, Titanium dioxide photocatalysis, *J. Photochem. Photobiol. C: Photochem. Rev.* 1 (2000) 1–21.
- [6] M.E. Davis, Ordered porous materials for emerging applications, *Nature* 417 (2002) 813–821.
- [7] A. Taguchi, F. Schüth, Ordered mesoporous materials in catalysis, *Microporous Mesoporous Mater.* 77 (2005) 1–45.
- [8] N.M. Julkapli, S. Bagheri, S.B.A. Hamid, Recent advances in heterogeneous photocatalytic decolorization of synthetic dyes, *Sci. World J.* 2014 (2014), doi: [10.1155/2014/692307](https://doi.org/10.1155/2014/692307) (Article ID 692307).
- [9] A. Mills, R.H. Davies, D. Worsley, Water purification by semiconductor photocatalysis, *Chem. Soc. Rev.* 22 (1993) 417–425.
- [10] S. Bagheri, N.M. Julkapli, S.B.A. Hamid, Functionalized activated carbon derived from biomass for photocatalysis applications perspective, *Int. J. Photoenergy* (2014) (Article ID 218743).
- [11] M.I. Litter, Heterogeneous photocatalysis transition metal ions in photocatalytic systems, *Appl. Catal. B* 23 (1999) 89–114.
- [12] N. Serpone, A.V. Emeline, Suggested terms and definitions in photocatalysis and radiocatalysis, *Int. J. Photoenergy* 4 (2002) 91–131.
- [13] S.D. Mo, W.Y. Ching, Electronic and optical properties of three phases of titanium dioxide: Rutile, anatase, and brookite, *Phys. Rev. B* 51 (1995) 13023–13032.

- [14] C. Xiaobo, Titanium dioxide nanomaterials and their energy applications, *Chin. J. Catal.* 30 (2009) 839–851.
- [15] A. Zaleska, Doped-TiO<sub>2</sub>: A review, *Recent Pat. Eng.* 2 (2008) 157–164.
- [16] M. Anpo, Use of visible light. Second-generation titanium dioxide photocatalysts prepared by the application of an advanced metal ion-implantation method, *Pure Appl. Chem.* 72 (2000) 1787–1792.
- [17] S. Bagheri, K. Shamel, S.B.A. Hamid, Synthesis and characterization of anatase titanium dioxide nanoparticles using egg white solution via sol–gel method, *J. Chem.* (2013) Article ID 848205, 5 pages.
- [18] H. Yamashita, M. Harada, J. Misaka, M. Takeuchi, Y. Ichihashi, F. Goto, M. Ishida, T. Sasaki, M. Anpo, Application of ion beam techniques for preparation of metal ion-implanted TiO<sub>2</sub> thin film photocatalyst available under visible light irradiation: Metal ion-implantation and ionized cluster beam method, *J. Synchrotron Radiat.* 8 (2001) 569–571.
- [19] T. Ohno, M. Akiyoshi, T. Umabayashi, K. Asai, T. Mitsui, M. Matsumura, Preparation of S-doped TiO<sub>2</sub> photocatalysts and their photocatalytic activities under visible light, *Appl. Catal. A* 265 (2004) 115–121.
- [20] S. Bagheri, N.M. Julkapli, S.B.A. Hamid, Titanium dioxide as a catalyst support in heterogeneous catalysis, *Sci. World J.* (2014) Article ID 727496, 21 pages.
- [21] J.C. Yu, L. Zhang, Z. Zheng, J. Zhao, Synthesis and characterization of phosphated mesoporous titanium dioxide with high photocatalytic activity, *Chem. Mater.* 15 (2003) 2280–2286.
- [22] S. Qourzal, A. Assabbane, Y. Ait-Ichou, Synthesis of TiO<sub>2</sub> via hydrolysis of titanium tetraisopropoxide and its photocatalytic activity on a suspended mixture with activated carbon in the degradation of 2-naphthol, *J. Photochem. Photobiol. A: Chem.* 163 (2004) 317–321.
- [23] E. Carpio, P. Zúñiga, S. Ponce, J. Solis, J. Rodriguez, W. Estrada, Photocatalytic degradation of phenol using TiO<sub>2</sub> nanocrystals supported on activated carbon, *J. Mol. Catal. A: Chem.* 228 (2005) 293–298.
- [24] Y. Li, X. Li, J. Li, J. Yin, Photocatalytic degradation of methyl orange by TiO<sub>2</sub>-coated activated carbon and kinetic study, *Water Res.* 40 (2006) 1119–1126.
- [25] Y.F. Lee, K.H. Chang, C.C. Hu, K.M. Lin, Synthesis of activated carbon-surrounded and carbon-doped anatase TiO<sub>2</sub> nanocomposites, *J. Mater. Chem.* 20 (2010) 5682–5688.
- [26] M. Asiltürk, Ş. Şener, TiO<sub>2</sub>-activated carbon photocatalysts: Preparation, characterization and photocatalytic activities, *Chem. Eng. J.* 180 (2012) 354–363.
- [27] M. Ouzzine, A.J. Romero-Anaya, M.A. Lillo-Ródenas, A. Linares-Solano, Spherical activated carbon as an enhanced support for TiO<sub>2</sub>/AC photocatalysts, *Carbon* 67 (2014) 104–118.
- [28] M.Q. Yang, N. Zhang, Y.J. Xu, Synthesis of fullerene-, carbon nanotube-, and graphene-TiO<sub>2</sub> nanocomposite photocatalysts for selective oxidation: A comparative study, *ACS Appl. Mater. Interfaces* 5 (2013) 1156–1164.
- [29] M.R. Mohammadi, M.C. Cordero-Cabrera, D.J. Fray, M. Ghorbani, Preparation of high surface area titania (TiO<sub>2</sub>) films and powders using particulate sol–gel route aided by polymeric fugitive agents, *Sens. Actuators B* 120 (2006) 86–95.
- [30] H.C. Choi, Y.M. Jung, S.B. Kim, Size effects in the Raman spectra of TiO<sub>2</sub> nanoparticles, *Vib. Spectrosc.* 37 (2005) 33–38.
- [31] K.V. Bineesh, D.K. Kim, D.W. Park, Synthesis and characterization of zirconium-doped mesoporous nano-crystalline TiO<sub>2</sub>, *Nanoscale* 2 (2010) 1222–1228.
- [32] N. Venkatchalam, M. Palanichamy, V. Murugesan, Sol-gel preparation and characterization of alkaline earth metal doped nano TiO<sub>2</sub>: Efficient photocatalytic degradation of 4-chlorophenol, *J. Mol. Catal. A: Chem.* 273 (2007) 177–185.
- [33] G. Soler-Illia, A. Louis, C. Sanchez, Synthesis and characterization of mesostructured titania-based materials through evaporation-induced self-assembly, *Chem. Mater.* 14 (2002) 750–759.
- [34] B.H. Stuart, *Infrared Spectroscopy: Fundamentals and Applications*, Wiley, Sydney, 2004, pp. 72–77.
- [35] A.J. Aishah, T. Sugeng, S.H. Adam, N.D. Rahim, M.A.A. Aziz, N.H.H. Hairom, N.A.M. Razali, M.A.Z. Abidin, M.K.A. Mohamadiah, Adsorption of methyl orange from aqueous solution onto calcined lapindo volcanic mud, *J. Hazard. Mater.* 181 (2010) 755–762.
- [36] M.M. Uddin, M.A. Hasnat, A.J.F. Samed, R.K. Majumdar, Influence of TiO<sub>2</sub> and ZnO photocatalysts on adsorption and degradation behaviour of erythrosine, *Dyes Pigm.* 75 (2007) 207–212.
- [37] S.K. Kansal, M. Singh, D. Sud, Studies on photodegradation of two commercial dyes in aqueous phase using different photocatalysts, *J. Hazard. Mater.* 141 (2007) 581–590.
- [38] V. Vimonses, S. Lei, B. Jin, C.W.K. Chow, C. Saint, Kinetic study and equilibrium isotherm analysis of congo red adsorption by clay materials, *Chem. Eng. J.* 148 (2009) 354–364.